Journal Name RSCPublishing

ARTICLE

Strong Antiferromagnetic Interaction in a 3D Copper-Organic Framework and Spin-glass-like Behaviour in a 1D Nickel Compound

Cite this: DOI: 10.1039/x0xx00000x

Received 00th January 2012, Accepted 00th January 2012

DOI: 10.1039/x0xx00000x

www.rsc.org/

Sheng-Yun Liao,[a] Tian-Hao Li,[a] Jin-Lei Tian,[a] Lin-Yan Yang,[a] Wen Gu,[a,b,*] and Xin Liu,[a,b,*]

The in situ hydrothermal reaction of 5-(4-carboxy-1*H*-1,2,3-triazol-1-yl) isophthalic acid (H_3ctia) with $M(NO_3)_2{\cdot}nH_2O$ (M = Cu, Ni) afforded two new coordination polymers, $\{[Cu_4(tia)_4(H_2O)_3]{\cdot}H_2O\}_n$ (**1**) and $\{Ni(H_2O)_6{\cdot}[Ni_2(ctia)_2(H_2O)_6]{\cdot}2H_2O\}_n$ (**2**) (tia^{2-} = 5-(1*H*-1,2,3-triazol-1-yl) isophthalate). X-ray structural analysis reveals complex **1** is an unusual 3D framework containing D_{4h} paddle-wheel copper units and two kinds of mononuclear copper units, and its resulting structure can be rationalized as a new topology with the Schläfli symbol of $\{4.8^2\}2\{4^2.8^5.10^6.12^2\}\{8^2.10\}2\{8^3\}2$. Compound **2** displays 1D zigzag chain structure. Strong antiferromagnetic interactions are observed among dinuclear units in complex **1**. Interestingly, complex **2** exhibits spin-glass-like behaviour with the spin glass freezing temperature at 15.8 K. In addition, the thermal stability of these compounds was also studied.

Introduction

The construction of coordination networks containing metal ions with magnetic anisotropy is particularly attractive owning to their aesthetic structure and potential application in the field of molecule-based magnetic materials[1]. However, the notion of effective design and synthesis of such materials has received less attention. When aiming to achieve such materials, the choice of appropriate bridging ligand and metal ions are of great importance.

So far, the majority of magnetic frameworks are the first row transition metals (Co, Ni and Cu) complexes[2]. That's because they have adjustable spin quantum number[3] and magnetic anisotropy[4].

As far as the ligand, the heterocyclic polycarboxylic such as pyridine-2,4-dicarboxylic acid[5], pyrazine-2,3-dicarboxylic acid[6], 1*H*-benzimidazole-5,6-dicarboxylic acid[7], isonicotinic[8], etc. were verified to be candidates due to their versatile coordination conformations and strong coordination ability. It has been demonstrated the mixed multiple heterobridges constructed by polydentate polyazole[9] and conformation-dependent carboxylate groups can efficiently mediate the different magnetic couplings with variable strength and nature[10]. H_3ctia is a new phenyl heterocyclic polycarboxylic ligand explored by our group and Guo[11] (see scheme 1). We selected phenyl heterocyclic polycarboxylic acid H_3ctia (see scheme 1) as the starting materials to assemble different paramagnetic ions to form metal-frameworks in consideration of the following points. (i) Two carboxyl groups and one triazol ring with one carboxyl group lie in meta-position, which may help construct the multi-dimensional structure. (ii) Short bridging such carboxyl and triazol bridging may be responsible for the formation of metal cluster. (iii) Long bridging across two aromatic rings may block the magnetic interaction among the clusters. Previously, a series of 3D Co-Ln heterometallic, 2D and 1D transition metal coordination polymers based on this ligand were reported[11]. Herein, we reported two new complexes, one 3D framework $\{[Cu_4(tia)_4(H_2O)_3]{\cdot}H_2O\}_n$(**1**) with strong antiferromagnetic interaction and one 1D chain $\{Ni(H_2O)_6{\cdot}[Ni_2(ctia)_2(H_2O)_6]{\cdot}2H_2O\}_n$(**2**) with spin glass behaviour.

Experimental

1 Materials and physical measurements

The reagents and solvents were obtained from commercial sources and used as received. Elemental analyses were determined on a Perkin-Elmer PE 2400 CHNS/O analyzer. IR spectra (KBr pellets) were recorded on a Perkin-Elmer spectrometer in the range 4000-400 cm^{-1}. Temperature- and field-dependent magnetic measurements were carried out on a SQUID-MPMS-XL magnetometer. Diamagnetic corrections were made with Pascal's constants. X-ray powder diffraction

(XRPD) intensities were measured on Rigaku D/max-IIIA diffractometer (Cu kα, λ = 1.54056 Å). The single crystalline powder samples were prepared by crushing the crystals and scanned from 3° to 6° with a step of 0.1°/s. Thermogravimetric analysis were performed on a NETZSCH TG 209 instrument with a heating rate of 10℃/min in the flowing air atmosphere.

2 General synthesis procedure

Synthesis of H_3ctia. H_3ctia was prepared according the literature[12] (yield: 70% based on 5-azidoisophthalic acid). ^{1}HNMR (300 Hz, DMSO-d_6, ppm): 8.02（s, 1H), 8.65 (s, 2H), 9.65 (s, 2H). IR (KBr pellets, cm^{-1}): 3129.6, 1723.9, 1545.2, 1475.0, 1414.0, 1331.0, 1255.4, 1188.2, 757.9, 712.1, 669.7 (see Fig S1 and S2 in supporting information).

Synthesis of $\{[Cu_4(tia)_4(H_2O)_3]\cdot H_2O\}_n$ (1). $Cu(NO_3)_2\cdot 3H_2O$ (48.2 mg, 0.2 mmol) and a solution of H_3ctia (16 mL, 0.02 mmol) whose pH value was adjusted to 3.5 by sodium hydrate was placed in a Teflon-lined autoclave and heated to 180℃ for three days, then cooled down to room temperature at a rate of 2.5℃/h. Blue block-shaped crystals suitable for X-ray analysis were directly obtained, collected, washed with water and dried in the air. Yield about 30% (based on $Cu(NO_3)_2\cdot 3H_2O$). Anal. Calcd (%) for $C_{40}H_{28}Cu_4N_{12}O_{20}$ (1250.90): C, 38.41%; H, 2.26%; N: 13.44%. Found: C, 38.50%; H, 2.2%; N, 13.44%. IR (KBr pellets, cm^{-1}): 3385, 1620, 1561, 1425, 1320, 1078, 787, 716.

Synthesis of $\{Ni(H_2O)_6\cdot[Ni_2(ctia)_2(H_2O)_6]\cdot 2H_2O\}_n$ (2). $Ni(NO_3)_2\cdot 6H_2O$ (0.058 g, 0.02 mmol) and a solution of H_3ctia (16 mL, 0.02 mmol) whose pH value was adjusted to 7.5 by sodium hydrate was placed in a Teflon-lined autoclave and heated to 160℃ for three days, then cooled down to room temperature at a rate of 2.0℃/h. Green block-like crystals suitable for X-ray analysis were obtained, washed with distilled water and dried in the air. Yield: 80% based on the $Ni(NO_3)_2\cdot 6H_2O$. Anal. calcd (%) for $C_{22}H_{36}N_6Ni_3O_{26}$ (976.70): C, 27.06%; H, 3.72%; N: 8.61%. Found: C, 27.31%; H, 3.68%; N, 8.62%. IR (KBr pellets, cm^{-1}): 3448, 1633, 1586, 1428, 1373, 1248, 1077, 772, 724 cm^{-1}.

3 X-ray structure determination of complexes 1−2

Diffraction data for complexes **1-2** were collected with a Bruker SMART APEX CCD instrument with graphite monochromatic Mo-Ka radiation (λ = 0.71073 Å). The data were collected at 293(2) K. The absorption corrections were made by multi-scan methods. The structure was solved by charge flipping methods with the program Olex2 and refined by full-matrix least-squares methods on all F^2 data with Olex2. The non-hydrogen atoms were refined anisotropically. Hydrogen atoms of water molecules were located in a difference Fourier map and refined isotropically in the final refinement cycles. Other hydrogen atoms were placed in calculated positions and refined by using a riding model. Crystallographic data for **1-2** are given in Table1. Selected bond lengths and angles are given in Tables S1-S2.

Table 1. Crystal data and structure refinement for **1** and **2.**

identification	Compound **1**	Compound **2**
formula	$C_{40}H_{28}Cu_4N_{12}O_{20}$	$C_{22}H_{36}N_6Ni_3O_{26}$
Mwt (g/mol)	1250.90	976.70
T (K)	273(2)	293(2)
crystal system	Triclinic	Triclinic
space group	$P\bar{1}$	$P\bar{1}$
a (Å)	10.3314(15)	6.958(2)
b (Å)	12.3196(18)	10.909(4)
c (Å)	19.042(3)	11.877(4)
α (deg)	106.785(3)	82.523(10)
β (deg)	93.694(3)	82.286(10)
γ (deg)	94.284(3)	71.561(9)
Z	2	1
ρ ($g\cdot cm^{-3}$)	1.803	1.922
μ (mm^{-1})	1.917	1.771
F (000)	1256	502
2θ scan range (°)	3.09 to 27.49	3.10 to 25.01
R_{int}	0.0485	0.0482
reflns collected	16474	5590
indep reflns	10233	2951
parameters	691	318
$R_1,\omega R_2$ [I>2σ(I)]	0.0679, 0.1774	0.0550, 0.1225
$R_1,\omega R_2$ [all data]	0.0946, 0.1952	0.0701, 0.1298
GOF on F^2	1.115	1.116
Largest residuals ($e\cdot Å^{-3}$)	1.409, -1.217	0.468, -0.568

Results and discussion

1 Conversion of H_3ctia

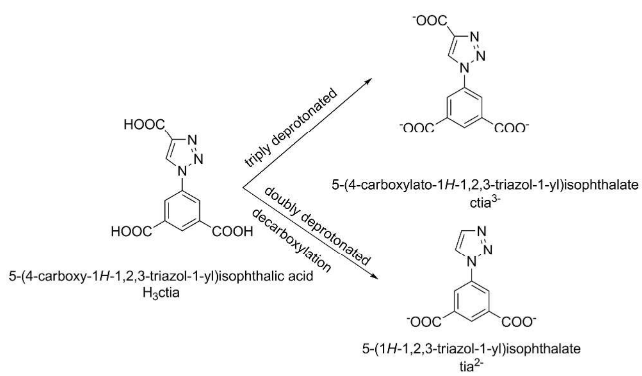

Scheme 1. Conversion of H_3ctia in construction of **1-2**.

Both target compounds were directly isolated by using 5-(4-carboxy-*1H*-1,2,3-triazol-1-yl) isophthalic acid (H_3ctia) as the starting materials. During the course of constructing **1**, H_3ctia underwent decarboxylation and doubly deprotonation to tia^{2-} (5-(1*H*-1,2,3-triazol-1-yl) isophthalate) (See Scheme 1). While in compound **2**, H_3ctia triply deprotonated to $ctia^{3-}$. Except for the reaction temperature and the pH of the solution, the other reaction conditions are the same, so these two factors may be responsible for the decarboxylation of H_3ctia in construction complex **1.**

2 Structure Descriptions

$\{[Cu_4(tia)_4(H_2O)_3]\cdot H_2O\}_n$ (1). Complex **1** is a 3 D metal-organic framework based on the D_{4h} paddle-wheel units

$[Cu_2(O_2CR)_4N_2]$ (see Figure 3(a)) which were connected by two kinds five coordinated monoclear Cu(II) units as linkers (Cu3 and Cu4, see Figure 1). Two kinds of μ_4-bridging ligand tia^{2-} (as designated infra with L^A and L^B, respectively, see Scheme 2) adopt four different modes to bridge Cu(II) centers (as designated infra with L^A , L^{B1}, L^{B2}, and L^{B3}, respectively, see Figure 2). In **2**, each $[Cu_2(O_2CR)_4N_2]$ dimer contains two antisymmetric Cu1 and Cu2 centers. Both of them take square-pyramid geometries, surrounded by four carboxylate O and one N donors from five distinct tia^{2-} ligands (one L^A, One L^{B1}, two L^{B2} and one L^{B3} for Cu1; Two L^A, One L^{B1}, one L^{B2} and one L^{B3} for Cu2) (see Figure 1 and Figure 2). The bond lengths and angles around Cu1 and Cu2 are similar. The bond length of Cu1-O and Cu2-O ranges from 1.941(4) to 2.019(4) Å and 1.929(4) to 1.980(4) Å, respectively. The bond length of Cu1-N and Cu2-N is 2.147(4) Å and 2.168(4) Å, respectively. The cis bond angles around Cu1 and the cis bond angles around Cu2 range from 87.80(17) to 101.69(17)° and 86.09(18) to 99.24(17) °, respectively. However, Cu3 and Cu4 adopt distorted trigonal bipyramid geometries. Cu3 is coordinated by O12 from the ligand L^{B2}, O16 from the ligand L^{B3}, N9 from the ligand L^{B3} and two water molecules (see Figure1). The bond lengths and cis angles around Cu3 range from 1.906(4) to 2.158(5) Å and from 86.99(18) to 127.3(3)°. Cu4 is coordinated by O3 and O4 from the ligand L^A, O8 and N6 from two ligands L^{B1} and one water molecule with the bond lengths and cis angles ranging from 1.910(5) to 2.010(5) Å and from 86.4(2) to 94.5(2)°. In **1**, the four carboxyl groups from the ligands L^A, L^{B1}, L^{B2} and L^{B3} bridge Cu1 and Cu2 to afford D_{4h} paddle-wheel units $[Cu_2(O_2CR)_4N_2]$[14] with a separation of 2.6339 Å (see Figure 3). These dinuclear units $[Cu_2(O_2CR)_4N_2]$, Cu3 and Cu4 ions are linked by L^A, L^{B1}, L^{B2} and L^{B3} to form 3D framework (Figure 3(b)). Compounds of the type $M_2(O_2CR)_4$ with D_{4h} paddle-wheel molecule structure are known for a variety of transition metals[13] such as Cu, Mo, Ru etc.

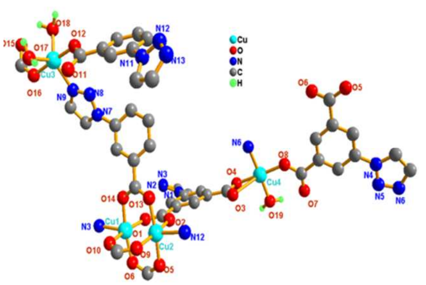

Figure 1 Local coordination environments of Cu(II) in **1.**

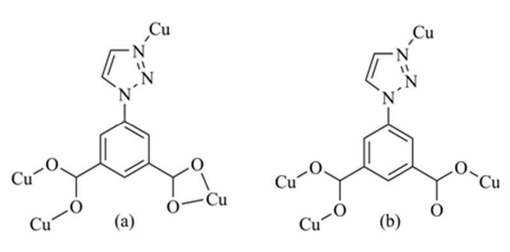

Scheme 2 Coordination modes of tia^{2-} in **1** (a) μ_4-Bridging: L^A; (b) μ_4-Bridging: L^B.

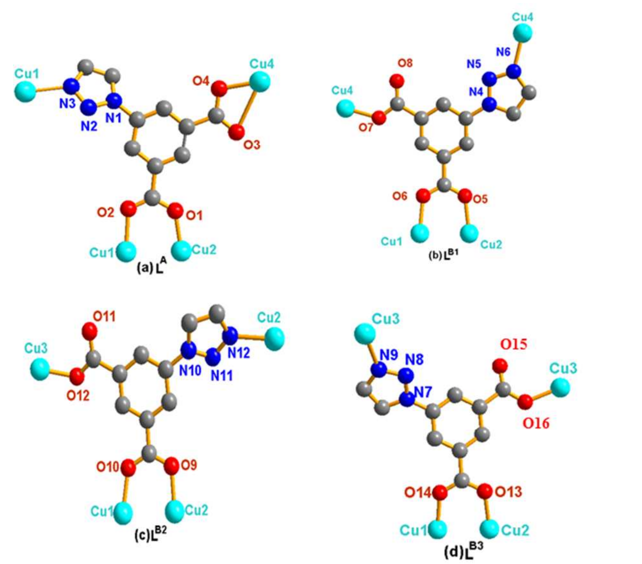

Figure 2 Bridging Cu(II) modes of the ligands tia^{2-}. (a) L^A: μ_4-Bridging; (b) L^{B1}: μ_4-Bridging; (c) L^{B2}: μ_4-Bridging; (d) L^{B3}: μ_4-Bridging.

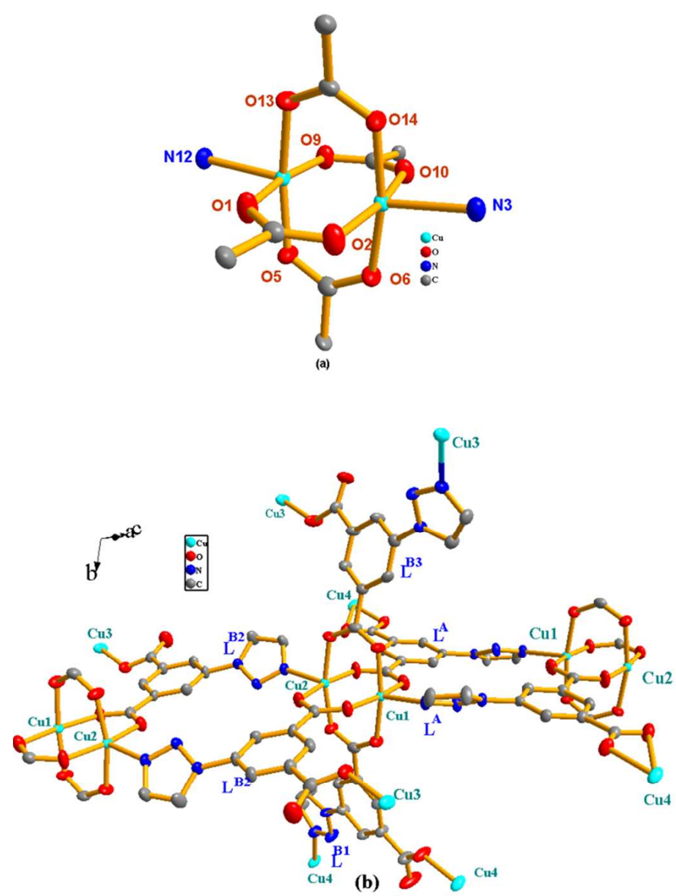

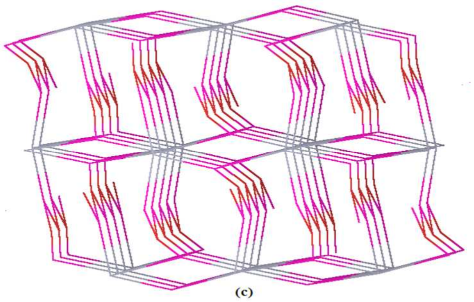

Figure 3. (a) paddle-wheel Cu(II) units; (b) Cu3 and Cu4 linked by the ligand tia^{2-} to form 3D framework. (c) Topologically representation for the 3D structure of **1**.

Better insight into this framework can be achieved by topology analysis. In **1**, the binuclear Cu(II) can be viewed as 6-connected nodes which are connected to two L^A, two L^{B2}, one L^{B1} and one L^{B3} ligands. While the Cu3, Cu4, the ligands L^A and L^B can be seen as 3-connected nodes (see Figure 3(c)). Therefore, this structure can be simplified as an unordinary 4-nodal (3,3,3,6)-connected topological network with the Schläfli symbol of $\{4.8^2\}2\{4^2.8^5.10^6.12^2\}\{8^2.10\}2\{8^3\}2$ {representing the ligand L^A and L^{B2}, binuclear Cu(II), L^{B1} and L^{B3}, mononuclear).

$\{Ni(H_2O)_6\cdot[Ni_2(ctia)_2(H_2O)_6]\cdot 2H_2O\}_n$ (**2**). Compound **2** has a 1D polymeric zigzag chain structure, which is similar to one Co(II) coordination polymer reported by Y. Li[15]. The asymmetric unit of **2** consists of two Ni(II) centers, one $Ni(H_2O)_6^{2+}$ cation and one independent $ctia^{3-}$ (Figure 4(a)). The Ni1 exhibits an octahedral coordination environment, where four oxygen atoms from the coordinated water molecules lie in the equatorial position and two O1 atoms from the symmetry-related ligands $ctia^{3-}$ with bond length of Ni1-O1, 2.026(3) Å. The Ni2 takes a distorted octahedral geometry with two O6 and two N3 atoms from the two symmetry ligands $ctia^{3-}$ on the equatorial position, while the apical position are occupied by two coordinated water molecules. As illustrated in Figure 4(b), the adjacent Ni ions are connected by the ligands $ctia^{3-}$ with a separation of 8.5701(22) Å, which is larger than the distance between them and their adjacent counter $Ni(H_2O)_6^{2+}$, to form a polymeric chain.

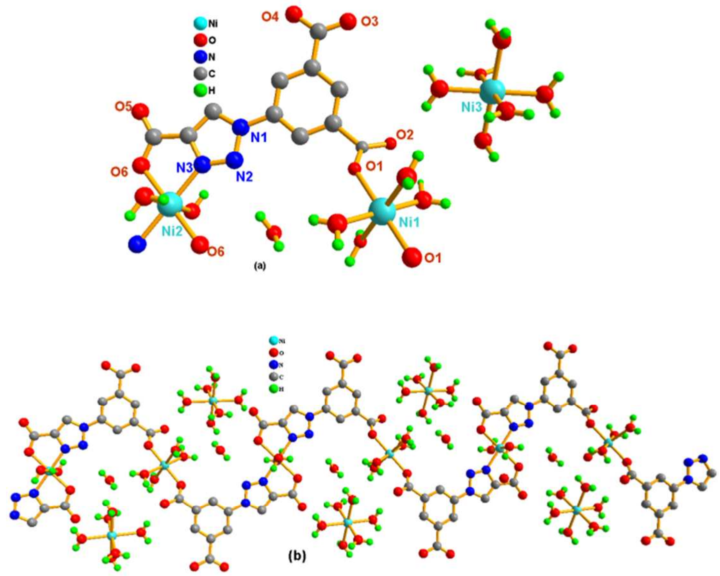

Figure 4. (a) ORTEP view of **2** with the thermal ellipsoids at 30 % probability showing the coordination environments of the Ni(II) atoms; (b) the 1D Ni(II) coordination chain.

3 XRPD results

X-ray powder diffraction measurements studies verify the as-obtained bulk substance of complexes **1** and **2** are homogeneous phase (see Fig.S3 in Supporting Information).

4 Magnetic properties

The magnetic properties of **1** and **2** were investigated in the 2.0-300 K range at 1000 Oe. The magnetic susceptibility of **1** versus temperature is shown in Figure 5. The $\chi_M T$ value is 0.94 cm^3 K mol^{-1} at 300 K, which is significantly smaller than the spin-only value of 1.5 cm^3 K mol^{-1} calculated for four Cu(II) ions (S = 1/2, g = 2). This suggests antiferromagnetic couplings exist between the paramagnetic ions even at room temperature. Upon lowering the temperature, the $\chi_M T$ decreases rapidly to 0.86 cm^3 K mol^{-1} from 300 K to 75 K, then keep constant until 15 K. when temperature continues to decrease, the $\chi_M T$ value slowly increases. The per mole magnetic susceptibility of **1**can viewed as sum of the contributions of one dinuclear Cu(II) unit and two free Cu(II) ions. The magnetic susceptibility of the dinuclear Cu(II) unit can be expressed by the Bleaney-Bowers equation. The χ_M of **1** is adequately represented by the equation (1).

$$\chi_M = \frac{Ng^2\beta^2}{T[3+\exp\left(\frac{-2J}{kT}\right)]} + 2\times\frac{N\beta^2}{3kT}[4S(S+1)] \qquad (1)$$

The least-squares fit to the data (60-300 K) leads to g =2.17, -2J = - 173.4 cm^{-1}, $R=\Sigma(\chi_{obsd}-\chi'_{cacld})^2/\Sigma(\chi_{obsd})^2 = 3.03\times10^{-4}$. Below 60 K, the data deviate substantially from the dimer model, presumably because of the presence of paramagnetic impurities.

From the view point of the relationship of magnetism and structure, the strong antimagnetic coupling of **1** mainly comes from paddle-wheel binuclear Cu(II) ions[16] bridged by tetracarboxyl groups with short distance of Cu1-Cu2. The drop in $\chi_M T$ to a value of 0.86 $cm^3\ K\ mol^{-1}$ at low temperature, which is very close to 0.75 $cm^3\ K\ mol^{-1}$ for two isolated Cu(II) with S = 1/2, g = 2, indicates the binuclear Cu(II) ions in the paddle-wheel units are strongly antiferromagnetically coupled to each other to a diamagnetic S = 0 ground state. When the temperature drops to 10 K, the $\chi_M T$ begins to increase slightly. That may be ascribed to the result of a minor paramagnetic impurity phase.[17].

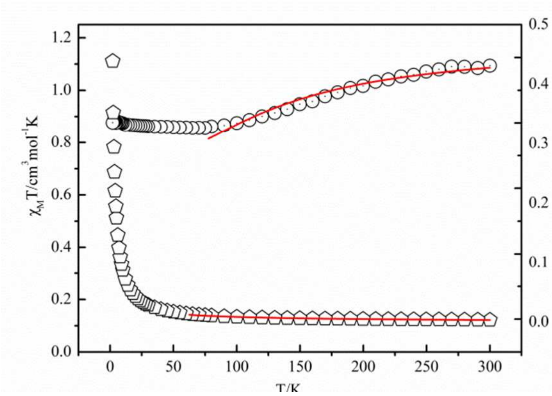

Figure 5 Temperature dependence of the $\chi_M T$ and χ_M^{-1} curve for **1**. The solid line represents the best fit.

As shown in Figure 6, complex **2** has a $\chi_M T$ value of 3.67 $cm^3\ K\ mol^{-1}$, which is close to the theoretical value of 3.3 $cm^3\ K\ mol^{-1}$ for S = 1 with g = 2.2[18]. Upon cooling from room temperature, the $\chi_M T$ value decrease from 3.67 to 3.48 $cm^3\ K\ mol^{-1}$ at ca. 40 K, which indicates a dominant antiferromagnetic interaction[19] between the Ni(II) ions. The magnetic susceptibility above 40 K obeys the Curie-Weiss law with Weiss constant, θ = − 4.23 K, and Curie constant, C = 1.141 $cm^3\ K\ mol^{-1}$. Then the $\chi_M T$ value increases rapidly to a maximum of 3.80 $cm^3\ K\ mol^{-1}$ at 26 K and finally drops to 2.05 $cm^3\ K\ mol^{-1}$.

The zero-field alternative-current (ac) magnetic susceptibility was performed under H_{ac} = 3.5 Oe and a frequency of 10-800 Hz (see Figure S4 in the supporting Information). Both of the in-phase and out-of-phase signals, χ_M' and χ_M'' display a very small frequency-dependent behaviour (see Figure S4 in the supporting Information and Fig S4'). The shift of the peak temperature (Tp) of χ_M' is measured by a parameter $\varphi = (\Delta Tp/Tp)/\Delta(\log f) = 0.01$, which is in the range of a spin-glass[21]. Unfortunately, the peaks of the out-of-phase are too small and close to the noise of the instrument, so the relaxation time (τ) and Δ/k_B can't be calculated from the Arrhenius law[22].

To further investigate the magnetic behaviour of **2** at low temperature, the field-cooled (FC) and zero-field-cooled (ZFC) magnetization measurements were performed at 50 Oe in the 2−30 K range (see Figure 7). The temperature correspondent to the ZFC maximum (15.8 K) is the spin glass freezing temperature.[20].

In addition, the field-dependent isothermal magnetization M(H) was performed at 2 K, a value of 4.8 $N\mu_B$ at 40 KOe is far below the saturation value of 6.6 $N\mu_B$ expected for the Ni_3 unit because of the spin glass component (see Figure S5 in the Supporting Information). Magnetization curve versus applied field measured at 2.0 K of Complex **2** did not exhibit an obvious hysteresis effect under our experimental conditions (Figure S5 in the Supporting Information: inset). Thus, it is difficult for us to further confirm the concrete magnetic behavior of **2.** But we can confirm complex **2** should be a spin glass.

Figure 6. Temperature dependence of the $\chi_M T$ and χ_M^{-1} curve for **2**. The solid line represents the Curie Weiss fit.

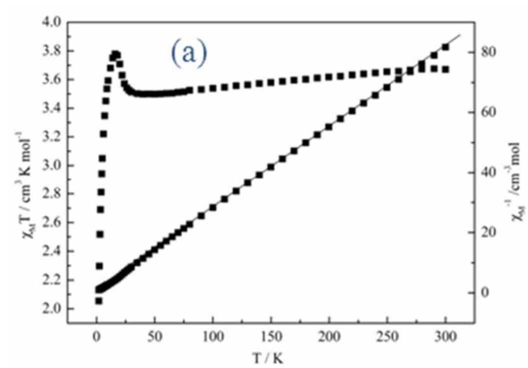

Figure 7. Field-cooled (FC) and zero-field-cooled (ZFC) magnetization plots of **2.**

5 Thermal Stability Properties

The TGA curve of **2** exhibits an initial weight loss from 100℃ to 30℃, with the observed weight loss of 25.3 % corresponding to the release of lattice and coordinated−water molecules (Calcd. 25.8%) (see Figure 8). After the water molecules were released, the skeleton collapse begins at about 300℃, which is lower than those of coordinated polymers reported previously[23]. That may be because complex **2** contains too much water molecules. The TGA diagram of complex **1** displays the loss of lattice water molecules at 170℃, which is higher than complex **2**. This can be ascribed to the fact that the three dimension framework can hinder the escape of the water molecules in some degree. Above 500℃, there is almost no weight loss in complexes **1** and **2**. The remnants of complexes **1** and **2** are 23.8% and 26.5%, respectively,

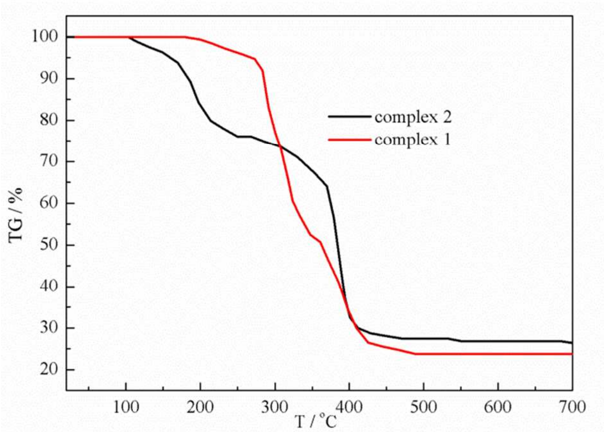

Figure 8. The TGA curves for complexes **1** and **2**.

Conclusions

In this contribution, we have presented two new metal−organic frameworks with the starting materials H_3ctia. Complex **1** is a 3D metal-organic framework based on the D_{4h} paddle-wheel units $[Cu_2(O_2CR)_4N_2]$ which were connected by two kinds five coordinated mononuclear Cu(II) units as linkers. Among the paddle-wheel units, the strong antiferromagnetic interaction can be observed between the Cu atoms. Compound **2** displays 1D zigzag chain structure. Interestingly, complex **2** exhibits spin-glass- behaviour with the spin glass freezing temperature at 15.8 K. Furthermore, the thermal stability of these compounds show the framework structure can affect the release of lattice water molecules.

Acknowledgements

This work was supported by the National Natural Science Foundation of China (No. 22371103 and No. 20771062) and the Tianjin Natural Science Foundation (No. 08JCZDJC21100).

Notes and references

[a] Department of Chemistry, Nankai University, Tianjin, China 300071
[b] Key Laboratory of Advanced Energy Material Chemistry, Tianjin, China 300071.

† Electronic Supplementary Information (ESI) available: Selected bonds and angles for **1** and **2**, powder X-ray diffraction patterns of **1** and **2**, Temperature dependence of ac susceptibility at various frequencies of **2** and Field dependence of magnetization and the hysteresis loop at 2 K for **2.** CCDC number 901576 and 901577 for **1** and **2.** For this ESI and crytallographic data in CIF and other electronic format see DOI: 10.1039/c0xx00000x

1 (a) J. W. Yoo, C. Y. Chen, H. W. Jang, C. W. Bark, V. N. Prigodin, C. B. Em and A. J. Epstein, *Nature Materials*, 2010, **9**, 638; (b) W. R. Entley, G. S. Girolami, *Science*, 1995, **268**, 397; (c) J. S. Miller, *Angew. Chem. Int. Ed.*, 2003, **42**, 47; (d) X. He, D. Antonelli, *Angew. Chem. Int. Ed.*, 2002, **41**, 214; (e) L. Bogani, L. Cavigli, M. Gurioli, R. L. Novak, M. Mannini, A. Caneschi, F. Pineider, R. Sessoli, M. Clemente-león, E. Coronado, A. Cornia and D. Gatteschi, *Adv. Mater.*, 2007, **19**, 3906. (f) J. S. Miller and M. Drillon, *Chem.Phys.Chem.*, 2002, **3**, 380; (g) M. Lopez, H. H. Zhao, A. V. Prosvirin, A. Chouai, M. Shatruk and K. R. Dumbar, *Chem. Commun.*, 2007, 4611; (h) M. Mito, K. Iriuchi, H. Deguchi and T. I. Kishine, *Physical Review B*, 2009, **79**, 012406; (i) R. Garde, F. Villain and M. Verdaguer, *J. Am. Chem. Soc.*, 2002, **124**, 1053; (j) S. I. Ohkoshi and K. Hashimoto, *J. Am. Chem. Soc.*, 1999, **121**, 1059.

2 (a) R. C. Poulten, M. J. Page, A. G. Algarra, J. J. Le Roy, I. López, E. Carter, A. Llobet, S. A. Macgregor, M. F. Mahon, D. M. Murphy, *J. Am. Chem. Soc.*, 2013, **135**, 13640-13643; (b) R. J. Kuppler, D. J. Timmons, Q.-R. Fang, J.-R. Li, T. A. Makal, M. D. Young, D. Yuan, D. Zhao, W. Zhuang, H.-C. Zhou, *Coord. Chem. Rev.*, 2009, **253**, 3042-3066; (c) W. Ouellette, A. V. Prosvirin, K. Whitenack, K. R. Dunbar, J. Zubieta, *Angew. Chem. Int. Ed.*, 2009, **48**, 2140-2143.(d) P. Jensen, S. R. Batten, B. Moubaraki, K. S. Murray, *Chem.commun.*, 2000, 793-794.

3 (a) Y.-Q. Lan, S.-L. Li, X.-L. Wang, K.-Z. Shao, D.-Y. Du, H.-Y. Zang, Z.-M. Su, *Inorg. Chem.*, 2008, **47**, 8179-8187; (b) L. R. MacGillivray, S. Subramanian, M. J. Zaworotko, *J. Am. Chem. Soc.*, 1994, 1325-1326; (c) R. Schenker, B. S. Mandimutsira, C. G. Riordan, T. C. Brunold, *J. Am. Chem. Soc.*, 2002, **124**, 13842-13855; (d) B. M. Weckhuysen, A. A. Verberckmoes, M. G. Uytterhoeven, F. E. Mabbs, D. Collison, E. de Boer, R. A. Schoonheydt, *The Journal of Physical Chemistry B.*, 2000, **104**, 37-42. (d) S. Yamaguchi, Y. Okimoto, H. Taniguchi, Y. Tokura, *Physical Review B*, 1996, **53**, 2926-2935.

4 (a) T. D. Harris, M. V. Bennett, R. Clerac, J. R. Long, *J. Am. Chem. Soc.*, 2010, **132**, 3980-3988; (b) J. H. Lim, J. H. Yoon, H. C. Kim, C. S. Hong, *Angew. Chem. Int. Ed.*, 2006, **45**, 7424-7426; (c) J. L. Manson, J. Gu, J. A. Schlueter, H.-H. Wang, *Inorg. Chem.*, 2003, **42**, 3950-3955; (d) M. A. Lawandy, X. Huang, R.-J. Wang, J. Li, J. Y. Lu, T. Yuen, C. Lin, *Inorg. Chem.*, 1999, **38**, 5410-5414.

(5) (a) M.-S. Liu, Q.-Y. Yu, Y.-P. Cai, C.-Y. Su, X.-M. Lin, X.-X. Zhou, J.-W. Cai, *Cryst. Growth Des.*, 2008, **8**, 4083-4091; (b) X. Wang, C. Qin, E. Wang, Y. Li, N. Hao, C. Hu, L. Xu, *Inorg. Chem.*, 2004, **43**, 1850-1856.

(6) (a) L.-L. Wen, Z.-D. Lu, X.-M. Ren, C.-Y. Duan, Q.-J. Meng, S. Gao, *Cryst. Growth Des.*, 2008, **9**, 227-238; (b) F.-Q. Wang, W.-H. Mu, X.-J. Zheng, L.-C. Li, D.-C. Fang, L.-P. Jin, *Inorg. Chem.*, 2008, 47, 5225-5233.

(7) (a) F. Stomeo, C. Lincheneau, J. P. Leonard, J. E. O'Brien, R. D. Peacock, C. P. McCoy, T. Gunnlaugsson, *J. Am. Chem. Soc.*, 2009, **131**, 9636-9637; (b) Y. Wei, Y. Yu, K. Wu, *Cryst. Growth Des.*, 2008, **8**, 2087-2089.

(8) (a) R. Sekiya, S.-i. Nishikiori, K. Ogura, *J. Am. Chem. Soc.*, 2004, 126, 16587-16600; (b) R. Sekiya, S. i. Nishikiori, *Chem. Eur. J.*, 2002, **8**, 4803-4810.

(9) (a) E.-C. Yang, Z.-Y. Liu, T.-Y. Liu, L.-L. Li, X.-J. Zhao, *Dalton Trans.*, 2011, **40**, 8132-8139; (b) Z.-G. Gu, Y.-F. Xu, X.-H. Zhou, J.-L. Zuo, X.-Z. You, *Cryst. Growth Des.*, 2008, 8, 1306-1312; (c)R. Bronisz, *Inorg. Chem.*, 2007, **46**, 6733-6739.

10 (a) Y. F. Zeng, X. Hu, F. C. Liu and X. H. Bu, *Chem. Soc. Rev.*, 2009, *38*, 469; (b) J. M. Rueff, N. Masciocchi, P. Rabu, A. Sironi and A. Skoulios, *Chem. Eur. J.*, 2002, **8**, 1813.

11 (a) S. Y. Liao, W. Gu, L. Y. Yang, T. H. Li, J. L. Tian, Li. Wang, M. Zhang and X. Liu, *Cryst. Growth Des.*, 2012, **12**, 3927; (b) S. Y. Liao, W. Gu, L. Y. Yang, T. H. Li, Li. Wang, M. Zhang and X. Liu, *Polyhedron*, 2012, **36**, 38-44; (c) Y. Li, W. Q. Zou, M. F. Wu, J. D.

Lin, F. K. Zheng, Z. F. Liu, S. H. Wang, G. C. Guo and J. S. Huang, *Cryst. Eng. Comm.*, 2011, **13**, 3868.

12 (a) P. Pierrat, S. Vanderheiden, T. Muller, S. Bräse, *Chem. Commun.*, 2009, 1748; (b) C. Camp, S. Dorbes, C. Picard and E. Benoist, *Tetrahedron Letters*, 2008, **49**, 1979-1983.

13 (a) Y. H. Shi, W. Z. Chen, K. D. John, R. E. D. Re, J. L. Cohn, G. L. Xu, J. L. Eglin, A. P. Sattelberger, C. R. Hare and T. Ren, *Inorg. Chem.*, 2005, **44**, 5719; (b) B. S. Kennon, J. H. Her, P. W. Stephens and J. S. Miller, *Inorg. Chem.*, 2009, **48**, 6117; (c) M. H. Chisholm, K. C. Glasgow, L. J. Klein, A. M. Macintosh and D. G.Peters, *Inorg. Chem.*, 2000, **39**, 4354; (d) F. A. Cotton, D. S. Martin, T. R. Webb and T. J. Peters, (e) D. S. Martin, R. A. Newman and P. E. Fanwick , *Inorg. Chem.*, 1979, **18**, 251;

14 (a) M.V. Marinho, M. I. Yoshida, K. J. Guedes, K. Krambrock, A. J. Bortoluzzi, M. Hömer, F. C. Machado and W. M. Teles, *Inorg. Chem.*, 2004, **43**, 1539; (b) S. Q. Su, Z. Y. Guo, G. H. Li, R. P. Deng, S.Y. Song, C. Qin, C. L. Pan, H. Guo, F. Cao, S. Wang and H. J. Zhang, *Daltons Trans.*, 2010, 3**9**, 3123.

15 Y. Li, W. Q. Zou, M. F. Wu, J. D. Lin, F. K. Zheng, Z. F. Liu, S. H. Wang, G. C. Guo and J. S. Huang, *Cryst. Eng. Comm.*, 2011, **13**, 3868.

16 (a) L. Gutiérrez, G. Alzuet, J. Borrás, A. Castiñeiras, A. Rodríguez-Fortea and E. Ruiz, *Inorg. Chem.*, 2001, **40**, 3089; (b) J. S. Valentine, A. J. Silverstein and Z. G. Soos, *J. Am. Chem. Soc.*, 1974, **96**, 97.

17 J. Garcia-Ruiz, J. Blasco, F. Hueso-Urena, M. Moreno-Carretero, *Journal of materials science*, 1998, **33**, 2103-2109.

18 D. K. Gao, Y. Z. Li and L. M. Zheng, *Inorg. Chem.*, 2007, **46**, 7571.

19 Y. Yafet, C. Kittel, Physical Review, 1952, **87**, 290.

20 (a)Y. G. Huang, D. Q. Yuan., L. Pan, F. L. Jiang, M. Y. Wu, X. D. Zhang, W. Wei, Q. Gao, J. Y. Lee, M. C. Hong, *Inorg. Chem.*, 2007, **46**, 9609; (b) M. R. Plout, S. Vilminot, M. Guillot and M. Kurmoo, *Chem. Mater.*, 2002, **14**, 3829.

21 (a) W. E. Buschmannn, J. Ensling, P. Gütlich and J. S. Miller, *Chem. Eur. J.*, 1999, **5**, 3019; (b) M. Arai, M. Miyake and M. Yamada, *J. Phys. Chem. C*, 2008, **112**, 1953; (c) G. Layrac, D. Tichit, J. Larionova, Y. Guari and C. Guérin, *J. Phys. Chem. C*, 2011, **115**, 3263; (d) J. Lefebvre, P. Tyagi, S. Trudel, V. Pacradouni, C. Kaiser, J. E. Sonier and D. B. Leznoff, *Inorg. Chem.*, 2009, **48**, 55.

22 (a) D. G. Branzea, L. Sorace, C. Maxim, M. Andruh and A. Caneschi, *Inorg. Chem.*, 2008, **47**, 6590. (b) K. C. Mondal, G. E. Kostakis, Y. H. Lan, C. E. Anson and A. K. Powell, *Inorg. Chem.*, 2009, **48**, 9205.

23 (a) D. Moon., J. Song, B. J. Kim, B. J. Suh and M. S. Lah, *Inorg. Chem*. 2004, **43**, 8230. (b) X. J. Gu and D. F. Xue, *Cryst. Growth Des.*, 2007, **9**, 1727.

Graphical abstract

Title: Strong Antiferromagnetic Interaction in a 3D Copper-Organic Framework and Spin Canting in a 1D Nickel Compound

Authors: Sheng-Yun Liao[a], Tian-Hao Li[a], Jin-Lei Tian[a], Lin-Yan Yang[a], Wen Gu [a,b,*], Xin Liu[a,b,*]

A novel 3D framework containing D_{4h} paddle-wheel copper units and 1D zigzag Nickel chain have been successfully synthesized and characterized magnetically.